

Pulsed Radiofrequency Relieves Neuropathic Pain by Repairing the Ultrastructural Damage of Chronically Compressed Dorsal Root Ganglion

Neuroscience Insights
Volume 20: 1–13
© The Author(s) 2025
Article reuse guidelines:
sagepub.com/journals-permissions
DOI: 10.1177/26331055251339081
journals.sagepub.com/home/exn



Xuelian Li¹, Ying Yang^{1,2}, Dong Huang^{1,3}, Jiahui Ma¹
and Yuzhao Huang^{1,4}

Abstract

Pulsed radiofrequency (PRF) has demonstrated therapeutic potential for neuropathic pain, yet its efficacy in alleviating pain induced by chronic dorsal root ganglion (DRG) compression remains unclear. This study evaluated the analgesic effects of DRG-targeted PRF in a chronic compression of DRG (CCD) rat model. Adult male Sprague Dawley rats were divided into four groups: sham, CCD, CCD+PRF, and CCD+freePRF. CCD was induced by inserting stainless-steel rods into the intervertebral foramen to compress L4/L5 DRGs. Pain behaviors, including spontaneous pain, mechanical/cold allodynia, and heat hypersensitivity, were assessed pre- and post-PRF treatment. On day 14 post-CCD, DRG ultrastructural changes and myelin basic protein (MBP) expression were analyzed via transmission electron microscopy and immunofluorescence. Compared to sham rats, CCD animals exhibited significant pain behaviors ($P < .0001$). PRF treatment in CCD+PRF rats significantly attenuated these behaviors ($P < .01$). Ultrastructural analysis revealed intact myelin sheaths in sham DRGs, whereas CCD DRGs showed myelin damage and reduced MBP expression ($P < .01$). Notably, PRF repaired myelin structural integrity and restored MBP levels. These findings demonstrate that DRG PRF alleviates neuropathic pain by reversing ultrastructural damage caused by chronic compression, providing mechanistic insights into PRF's analgesic effects and supporting its therapeutic value for neuropathic pain management.

Keywords

pulsed radiofrequency, neuropathic pain, chronic compression of dorsal root ganglion, ultrastructural damage, neuromodulation

Received: 18 December 2024; accepted: 16 April 2025

¹Department of Pain, The Third Xiangya Hospital and Institute of Pain Medicine, Central South University, Changsha, China

²Hunan Key Laboratory of Nanophotonics and Devices, Hunan Key Laboratory of Super-Microstructure and Ultrafast Process, School of Physics, Central South University, Changsha, China

³Hunan Key Laboratory of Brain Homeostasis, Central South University, Changsha, China

⁴Department of Orthopedics, The Third Xiangya Hospital, Central South University, Changsha, China

#Contributed equally.

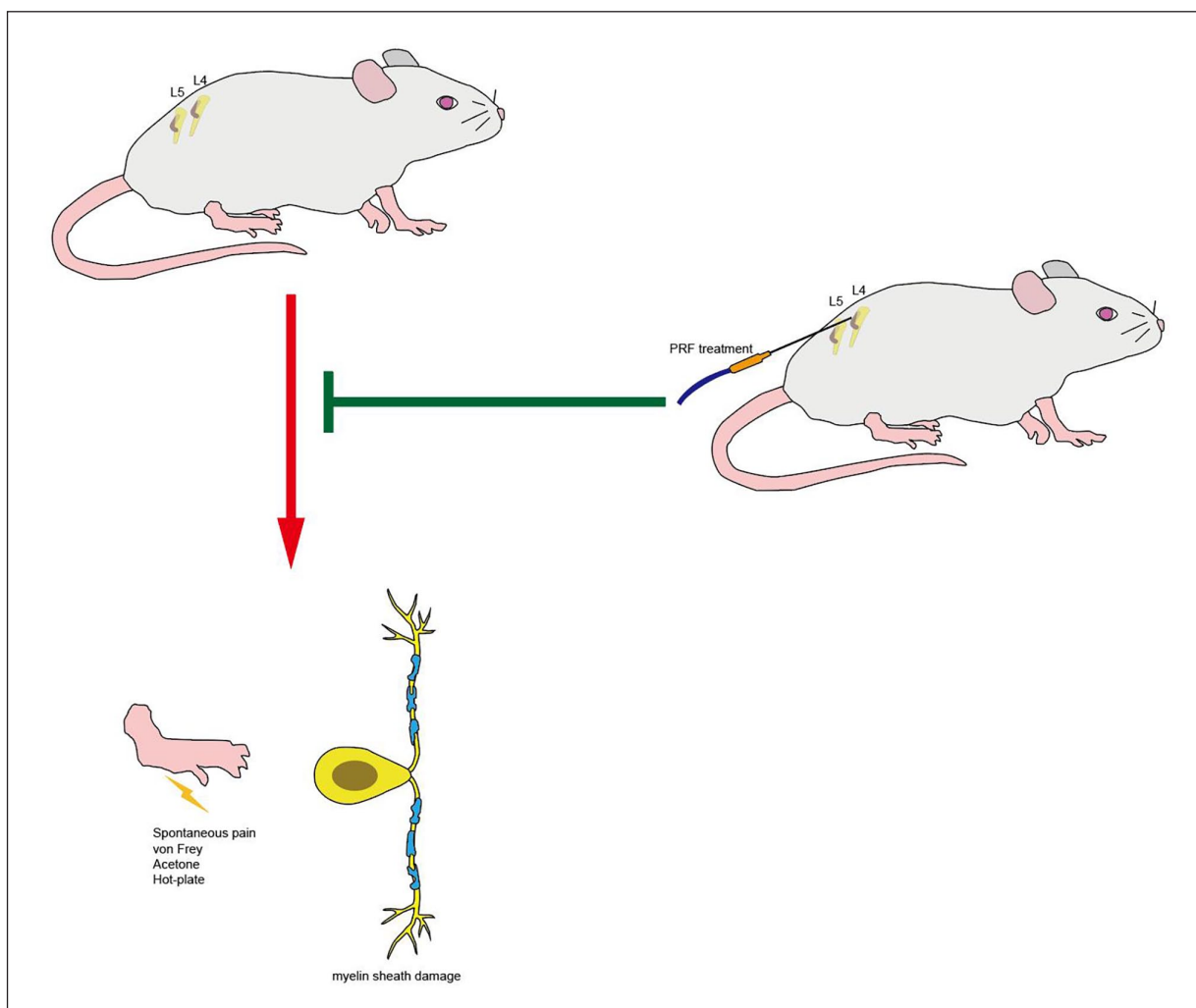
Corresponding authors:

Jiahui Ma, Department of Pain, The Third Xiangya Hospital and Institute of Pain Medicine, Central South University, Changsha, 410013, China.
Email: 531188643@qq.com

Yuzhao Huang, Department of Pain, The Third Xiangya Hospital and Institute of Pain Medicine, Central South University, Changsha, 410013, China.
Email: hyzxiangya3@outlook.com



Graphical abstract



Introduction

According to the International Association for the Study of Pain (IASP), neuropathic pain (NeP) is described as pain caused by a lesion or disease of the somatosensory system.¹ The estimate of the prevalence of pain with neuropathic characteristics is about 6.9% to 10% of the population.²⁻⁴ Doth et al. reported that patients with NeP (painful radiculopathy, failed back surgery) have a higher health burden compared to some major diseases (diabetes, heart failure and Parkinson's disease).⁵ Although many treatment modalities have been reported for NeP, the available evidence is insufficient to allow recommendations about the optimal therapy. Pharmacologic treatment remains the first choice for the management of lumbosacral radicular pain, including antidepressants (tricyclic agents and serotonin-norepinephrine reuptake inhibitors) and anticonvulsants (gabapentin and pregabalin). Patients with NeP may not respond adequately to pharmacologic treatments. It is

necessary to consider interventional strategies before patients continue endless pharmacological rotation that does not produce satisfactory pain relief or induce intolerable adverse effects.^{6,7} Techniques of interventional pain management include nerve block, intrathecal medication, pulsed radiofrequency (PRF), spinal cord stimulation and neurosurgical interventions. Recently, PRF has been increasingly recommended in the management of different neuropathic conditions, including postherpetic neuralgia, radicular pain and trigeminal neuralgia.⁸⁻¹⁰

PRF aims to modulate a nerve to provide pain relief. It creates an electrical circuit and generates heat with the target tissue, then delivers in an intermittent fashion and induces changes in the neuronal cells.¹¹ PRF may have an effect on the synaptic transmission or excitability of nerve fibers, especially small-diameter A δ and C-fibers. PRF presents an anti-inflammatory effect, which may impact immune cells and proinflammatory cytokines.^{12,13} An electroporation-mediated calcium influx is also involved in the

pathophysiology of PRF.¹⁴ Due to the critical role played by dorsal root ganglion (DRG) neurons in the induction and maintenance of chronic pain, it has been a new pharmacological and neurostimulator technological target for pain management.^{15,16} Jiang et al. showed that PRF treatment either to DRG or to the sciatic nerve can reduce neuropathic pain behavior in CCI (chronic constriction injury) rats, but PRF to DRG had a better analgesic effect than PRF to the nerve.¹⁷ Although DRG PRF is becoming an alternative option, its underlying neurophysiological mechanism is still limited.

To improve existing treatments for neuropathic pain, it is of pivotal importance to explore the cellular and molecular changes induced by PRF. There are several animal models for studying pain paradigms and related mechanisms. The surgical approach of sciatic or peripheral nerve ligation/transection represents well-validated models to reproduce neuropathic pain following PNS damage, while injuries to herniated discs and spinal or foraminal stenosis can cause radicular pain.¹⁸ The efficacy of DRG PRF has been identified in models of peripheral nerve injury, such as the CCI and SNI (spared nerve injury) models, but it has not been used in the animal model of lumbosacral radicular pain caused by DRG injury.¹⁷⁻¹⁹ The typical animal model of low-back and lumbosacral radicular pain is the CCD model. It is a key to solve the position relationship between the tip of the electrode and compressed rods during PRF treatment. Thus, one purpose of this study was to explore the efficacy of DRG PRF in CCD rats. In addition, in order to provide basic evidence for its neurophysiological mechanism, we also explored the DRG PRF effect on the ultrastructural change in the DRG.

Materials and Methods

Animals

The study was conducted under the approval of the Laboratory Animal Ethics Committee of Central South University (NO. 2022-0042). Twenty-eight healthy male adult Sprague Dawley rats (aged 8-10 weeks, 200-250 g) were reared under standard conditions, namely 12 h: 12 h circadian cycle, room temperature 23 ± 2 °C, humidity 50%-60% and free access to food and clean water. The experiment started after one week of adaptive feeding. Rats were randomized into sham, CCD, CCD+PRF and CCD+freePRF groups, with 7 rats in each group.

Chronic Compression of DRG (CCD)

The rats were anesthetized with a combination of pentobarbital (40 mg/kg, i.p.) and sevoflurane (1%, inhalation). Hair was removed from the surgical area. The incision was defined according to the bony marks of the iliac crest. Referring to the method of Song et al.²⁰, stainless-steel rods were inserted into the intervertebral foramina. In brief, guided by the anatomical position of the transverse and articular processes, L-shaped stainless-steel rods 4 mm in

length and 0.8 mm in diameter were inserted into intervertebral foramina to compress the L4 and L5 DRGs at a rostral direction at an angle of 30-40° to the dorsal middle line and -10 to -15 below the vertebral lateral horizontal line. When the rod was inserted, the rat's right hind limb could be seen to twitch slightly 1-2 times. After confirming the position of the rods, the muscle and skin were sutured layer-by-layer. Figure 1 shows the anatomy (Figure 1a) and X-ray (Figure 1b and c) of the placed stainless-steel rods. In the sham group, the procedure was the same as above, but only the foramina were exposed and no rod was placed.

Pain Behavior Tests

Order of Tests. On each test day, the rats were brought into the behavioral chamber 1 hour earlier to allow for acclimatization, and the room temperature was maintained at 22-24 °C. Each test was performed by the same tester, who was blinded to the grouping of rats. The order of tests was uniform for each rat, with behavioral tests performed starting from the test with minimal stimulation so as to minimize the effect that one test caused on the next, in the order of (1) withdrawal of hind paw ipsilateral to chronic compression DRG in normal condition; (2) 50% mechanical paw withdrawal threshold (MPWT); (3) acetone response score; and (4) thermal paw withdrawal threshold (TPWT). The interval between each behavior test was more than 30 minutes.

Spontaneous Pain. The rats were habituated in a transparent box (25*30*25 cm) for at least 20 minutes before testing. The plantar behavior of each rat was recorded with a high-resolution camera (Qianshiyan Technology Company, Shenzhen, China) at 30 frames per second for 30 minutes. The frequency of spontaneous pain of the right hind paw (lifting, licking, flinching or biting) was analyzed before the modeling and 2 weeks after the surgery.²¹

Mechanical Paw Withdrawal Threshold (MPWT) of 50%. After the rats were acclimated to a transparent box with metal meshes at the bottom, a von Frey hair (North Coast, US) was used in a gradient from small to large (0.4, 0.6, 1.0, 1.4, 2.0, 4.0, 6.0, 8.0, 10.0, 15.0 gram) according to the up-and-down method described by Dixon.²² Through the metal mesh, the right midplantar region of the rat was carefully stimulated manually using von Frey hair. The hair was kept bent for 5 seconds to observe the paw withdrawal response of the rats. After the first paw retraction, the rats were continuously measured 6 times, with more than 30 seconds between each stimulus, and the sequence of the 6 stimuli and the value of the von Frey hair at the last time were recorded. The 50% MPWT was calculated from the test results using the method of Chaplan et al.²³ The tests were performed 1 day before stainless-steel rod implantation and 5, 7, 8, 11, 14, 18, 23 and 28 days after surgery.

Acetone Evaporation Test. The rats were placed in a transparent box with metal meshes at the bottom. After the rats

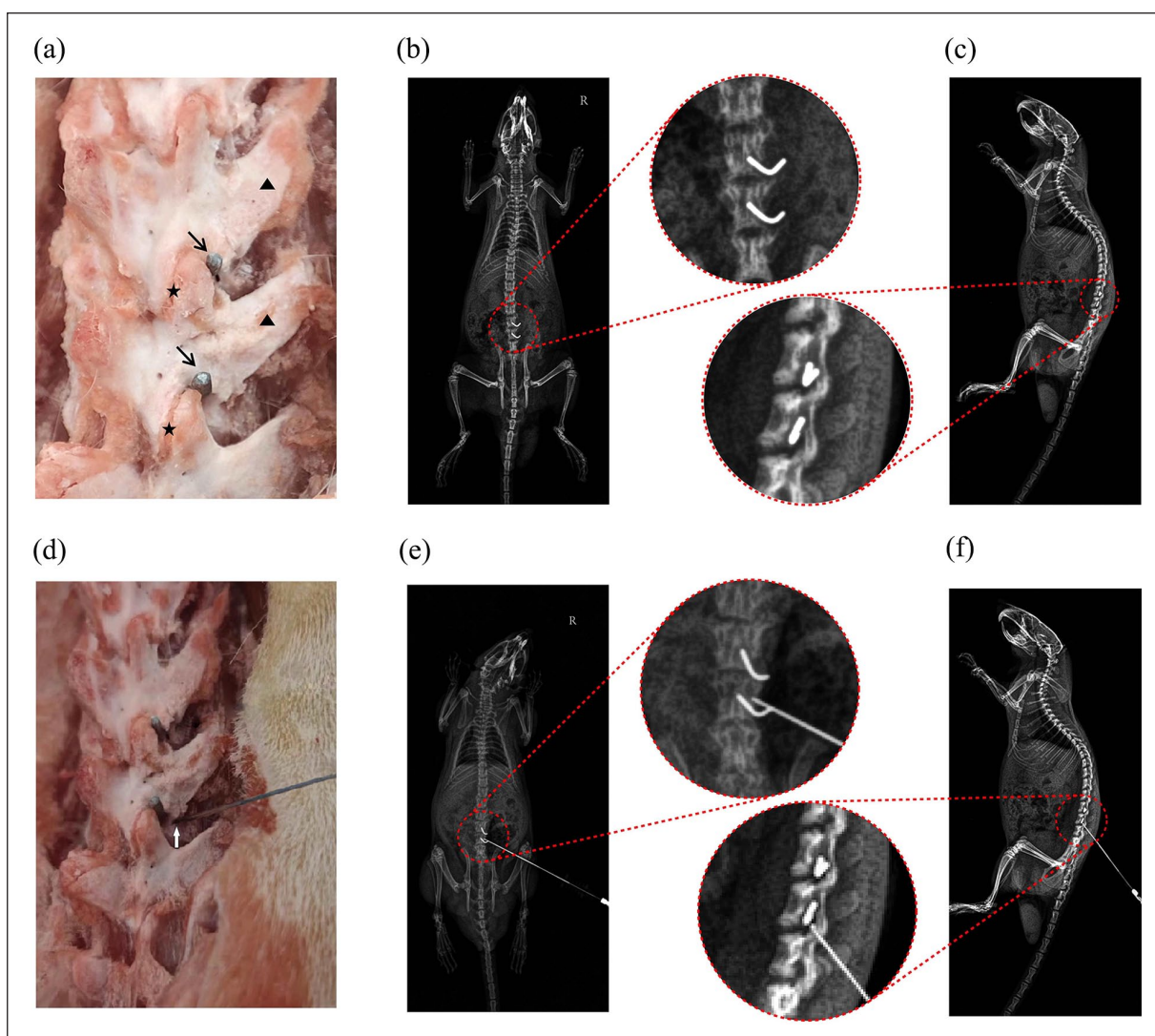


Figure 1. Anatomy and X-ray shows the position of the stainless-steel rods in the intervertebral foramina and the position of electrode during PRF treatment: (a) Anatomy of the lumbar vertebrae with stainless-steel rods. ▲ Transverse processes of L4 and L5; ★ Facet joints; ↘ Stainless-steel rods, (b) Anterior–posterior radiograph of the implanted stainless-steel rods, (c) Lateral radiograph of the implanted stainless-steel rods, (d) Anatomy of the position of electrode during PRF treatment. The white arrow indicates the tip of the electrode, (e) Anterior–posterior radiograph of the position of electrode during PRF treatment, and (f) Lateral radiograph of the position of electrode during PRF treatment.

were acclimated, quantitative acetone was gently applied to the right plantar of the rats as described by Silva-Cardoso et al.²⁴ and Yoon et al.²⁵ The rats' responses were observed and graded according to the following scores: 0 (no response); 1 (brisk withdrawal or flick of the paw); 2 (repeated flicking of the paw); 3 (repeated flicking of the hind paw and licking of the paw). A high score represents cold allodynia. Five experiments were performed for each rat with an interval of more than 5 minutes. The average score of the five measurements was used as the result of the cold pain measurement. The tests were performed 1 day before stainless-steel rod implantation and 5, 7, 8, 11, 14, 18, 23, and 28 days after surgery.

Hot-plate Test. According to the established methods,²⁶ the temperature of the hot plate (Shanghai Yuyan, BME-480, Shanghai, China) was controlled at $50 \pm 0.2^\circ\text{C}$, and a

transparent box was placed on the hot plate to restrict the rats to moving only on the hot plate. The time from the right plantar contact with the hot plate to the first response (licking, jumping and rapid paw withdrawal) was recorded. The cut-off time was set at 20 seconds to avoid tissue damage. A total of 5 measurements were taken with an interval of more than 20 minutes. The average time of the five measurements was taken as the thermal paw withdrawal threshold (TPWL). The tests were performed 1 day before stainless-steel rod implantation and 5, 7, 8, 11, 14, 18, 23, and 28 days after surgery.

PRF on DRG

For the CCD+PRF group, PRF was applied to the L4 and L5 dorsal root segments of the operated side through the intervertebral foramen 7 days after the establishment of the

CCD model. After the rats were anesthetized, the L4 and L5 foramina where the stainless-steel rods were placed were surgically exposed. A 50mm, 20 G catheter needle with active tip electrode was placed at the intervertebral foramen, avoiding direct contact with the rod, and then tested to have a tissue impedance of less than 200 Ω . Muscle contractions were tested using electrical stimulation at 4Hz with a maximum output voltage of 1.0 V. When muscle contractions were observed at a voltage of less than 0.8 V, the needle was withdrawn for 1 mm. When the voltage was greater than 1.0 V and no muscle contraction was observed, the needle was inserted for 1 mm. The above steps were repeated until muscle contractions could be observed at output voltages of 0.8 to 1.0V. This criterion can ensure that the electrodes are close to the DRG but do not damage it during treatment. According to treatment parameters used by our team for lumbosacral radicular pain, pulsed radiofrequency was performed at 2Hz, 20ms pulse width, a voltage of 70 V and a maximum temperature of 48°C, with each DRG treated 3 times for 240seconds each time, using standard clinical-specification radiofrequency generator (Beiqi, R-2000BA1, Beijing, China).⁹ The position of the electrode tip was kept fixed during treatment. After PRF treatment, the electrodes were removed, and the muscle and skin were sutured. Figure 1 shows the anatomy (Figure 1d) and X-ray (Figure 1e and f) of the position of the electrode during PRF treatment. The CCD+freePRF group underwent the same procedure as above but without pulse electrical stimulation.

Transmission Electron Microscopy Analysis

On the 14th day post-surgery, the DRGs were removed to observe their myelinated nerve fibers using transmission electron microscopy after all the behavioral tests. Specifically, in order to obtain relatively objective and standardized results, DRG specimens from all animals were given to the same pathologist, who was blind to the study groups. The specimens were fixed, dehydrated, embedded and sectioned by the pathologist, and the ultrastructure of the specimens was observed and scored according to the myelin ultrastructure evaluation method: 0 (Normal myelin layers); 1 (Vesiculated myelin); 2 (Cracked myelin layers); 3 (honeycomb & extruded vesicles).²⁷ Higher scores indicated more severe ultrastructural damage.¹⁰ Images were randomly captured by the pathologist from each group, with each image magnified 10,000 times. From these images, twenty myelin sheaths were randomly selected for assessment of structural damage scoring. When more than one grade of damage was presented in the same myelin sheath at the same time, the score corresponding to the most severe injury was taken.

Immunofluorescence

Following deep anesthesia with pentobarbital (40 mg/kg, i.p.) and sevoflurane (1%, inhalation), rats underwent

transcardial perfusion with 0.9% saline followed by 4% paraformaldehyde (PFA) in 0.1 M phosphate buffer (PB, pH 7.4). L4 and L5 DRG were dissected and post-fixed in 4% PFA for 24hours at 4°C, then cryoprotected in 30% sucrose solution until tissue saturation. Cryosections (30 μ m thickness) were obtained using a Leica CM1950 cryostat (-20°C chamber temperature) and collected in 0.01 M phosphate-buffered saline (PBS, pH 7.4) for free-floating Immunofluorescence. Followed by permeabilization with 0.3% Triton X-100 in PBS. Non-specific binding was blocked using 5% bovine serum (Servicebio, GC305010) in PBS for 1 hour at room temperature(RT). Sections were incubated with primary antibody against myelin basic protein (MBP, mouse monoclonal, GeneTex, GTX634292, 1:200 in PBS) for 12hrs at 4°C. After 3*10 minutes PBS washes, sections were treated with Alexa Fluor 594-conjugated donkey anti-mouse IgG (1:200, Servicebio,GB28303) for 1hr at RT. After 3*10 minutes PBS washes, nuclei were counterstained with DAPI (Sigma-Aldrich D9542). Sections were mounted on Superfrost Plus slides (Thermo Fisher) using ProLong Diamond antifade mountant (Invitrogen P36961). Images were acquired using fluorescence microscopy (Zeiss). MBP immunoreactivity was quantified as a percentage positive area using ImageJ 1.53t with consistent thresholding across all samples.

Statistical Analysis

Two-way ANOVA with repeated measures and Bonferroni's post-test were used to compare the statistical differences of 50% MPWT, acetone response score and TPWT over time in each group. Chi-square was used to compare differences in the distribution rates of myelin sheath scores. The difference in immunofluorescence positive staining area was compared using an unpaired *T* test. Graphpad Prism 8 (US) was used for statistical analysis, and the significance level was $P < .05$.

Results

The CCD Model Induced Neuropathic Pain

After establishing the CCD model and performing pain behavior tests, we found that compared with the sham group, the rats in the CCD group showed significant spontaneous pain (Figure 2a, $P < .0001$), mechanical allodynia (Figure 2b, $P < .0001$), cold allodynia (Figure 2c, $P < .0001$) and heat hyperalgesia (Figure 2d, $P < .0001$).

Chronic Compression of DRG Results in Ultrastructural Damage

Transmission electron microscopy analysis revealed distinct ultrastructural alterations in compressed DRG. In the sham group, myelinated nerve fibers predominantly exhibited structural integrity with continuous lamellar arrangements, though focal vesicular alterations were occasionally

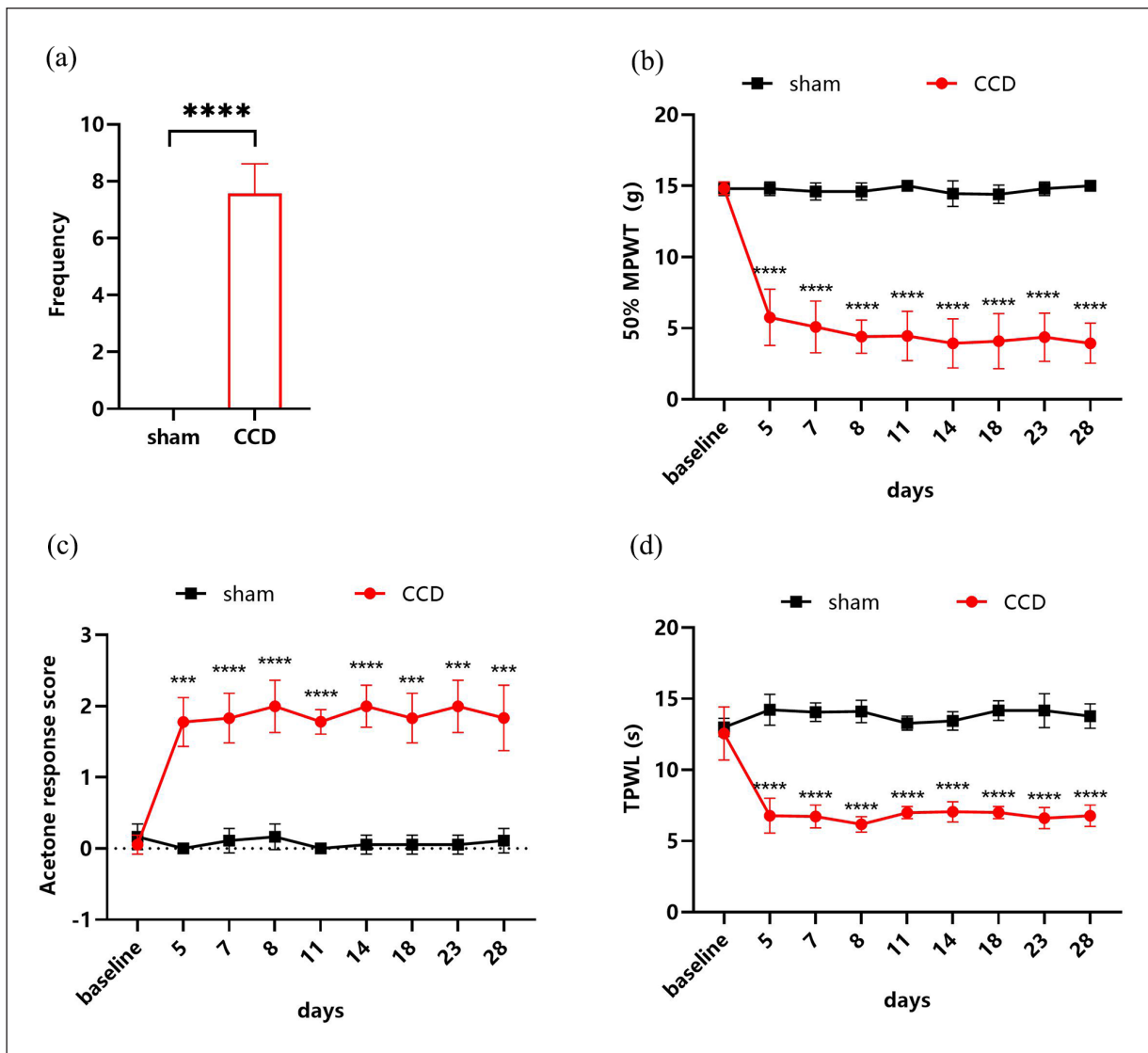


Figure 2. The CCD model induced persistent neuropathic pain. (a) CCD rats showed significant spontaneous pain. $P < .0001$; $N = 7/7$; unpaired t -test, (b) Rats displayed mechanical allodynia after establishment of CCD. $F(8, 96) = 31.02$; $P < .0001$; $N = 7/7$, Two-way ANOVA with repeated measures and Bonferroni's post-test, (c) The acetone response scores of CCD rats were significantly increased. $F(8, 96) = 34.84$; $P < .0001$; $N = 7/7$, Two-way ANOVA with repeated measures and Bonferroni's post-test, (d) The CCD model resulted in a significant decrease in the thermal paw withdrawal latency of rats $F(8, 96) = 25.07$; $P < .0001$; $N = 7/7$, Two-way ANOVA with repeated measures and Bonferroni's post-test. *** $P < .001$, **** $P < .0001$. MPWT, mechanical paw withdrawal latency; TPWL, thermal paw withdrawal latency.

observed in localized myelin regions (Figure 3a and b). In contrast, CCD group specimens demonstrated significant myelin derangements characterized by three predominant pathological features: (1) widespread vesiculation disrupting lamellar continuity, (2) segmental myelin fragmentation with lamellar separation, and (3) honeycomb-like decompaction patterns accompanied by axoplasmic extrusion (Figure 3c and d). Quantitative assessment using a standardized myelin injury grading system confirmed substantially greater structural compromise in the CCD group compared to sham controls (Figure 4, $P < .0001$). Immunofluorescence analysis provided complementary molecular evidence for

myelin pathology. Analysis of the MBP positive area in DRG sections revealed a significantly lower expression level in the CCD group compared with the sham group (Figure 5, $P < .01$).

DRG PRF Relieves Neuropathic Pain in CCD Rats

We performed PRF on the DRGs of rats with neuropathic pain. The results of pain behavior tests after PRF treatment showed that PRF attenuates spontaneous pain (Figure 6a, $P < .05$), mechanical allodynia (Figure 6b, $P < .01$), cold

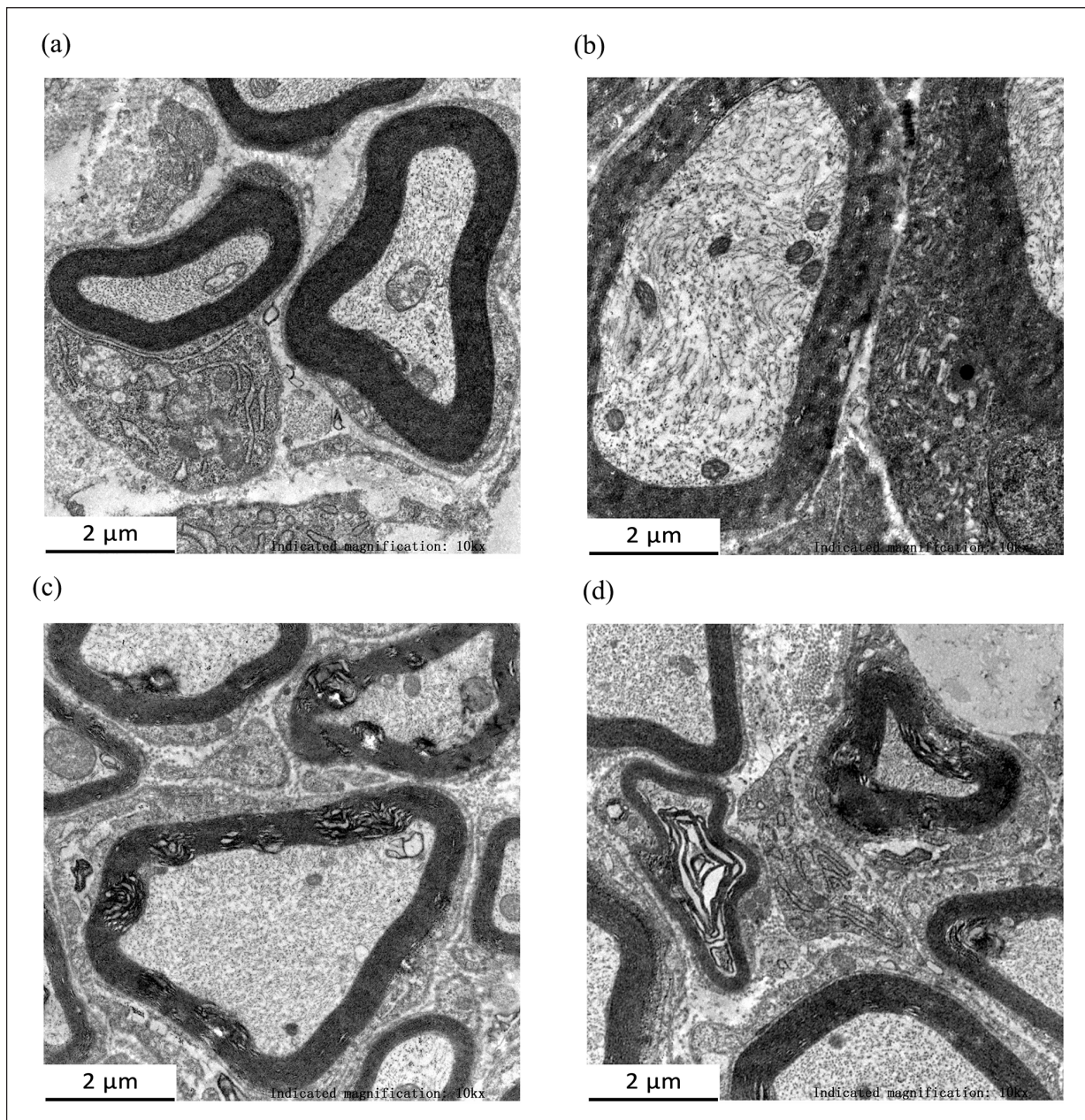


Figure 3. Ultrastructural changes of DRG in the sham and CCD groups. In the sham group, the myelin sheath of myelinated nerve fibers was basically intact (a). Only a few vesicles appeared (b). In contrast, the myelin sheath of the CCD group showed vesicles, stratification, fracture or collapse into a honeycomb (c, d). Scale bar = 2 μm ; magnification *10,000.

allodynia (Figure 6c, $P < .001$), and heat hyperalgesia (Figure 6d, $P < .01$) in CCD rats.

Repair Effect of PRF on Ultrastructural Damage of DRGs in CCD Rats

We further observed the effect of PRF on the ultrastructure of DRGs in CCD rats, and the results showed that compared with the CCD+freePRF group, the myelin damage in the CCD+PRF group was repaired to a certain extent, including reduced vesicles and layered myelin repair (Figure 7). In addition, the comparison results of myelin damage grading also showed that PRF had a significant improvement effect on the ultrastructural

damage of DRG in CCD rats, and the scores of the PRF group were significantly reduced (Figure 8, $P < .05$). Immunofluorescence results also showed that MBP expression in DRG of CCD+PRF group was up-regulated after PRF treatment compared with CCD+free-PRF group (Figure 9, $P < .05$).

Discussion

As a general medical therapy, pulse radiofrequency is used for various painful states in clinical practice. Many studies have demonstrated the effectiveness of applying PRF to DRGs in neuropathic pain.^{15,28,29} In the present study, we investigated the effects of DRG PRF treatment

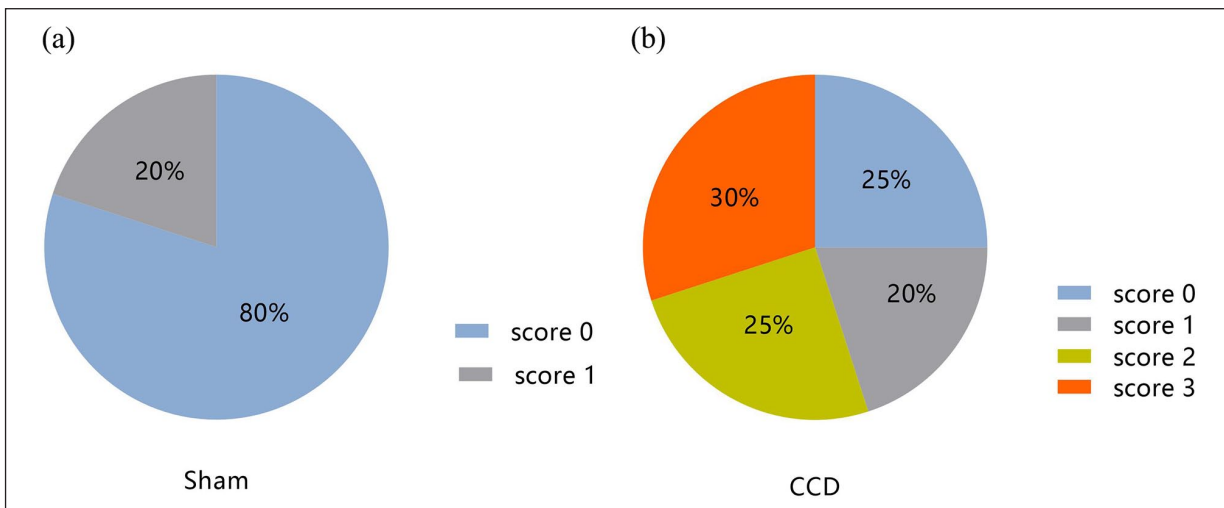


Figure 4. Ultrastructural scores of the sham group (a) and CCD group (b). $N=20$; $P < .0001$, Chi-square.

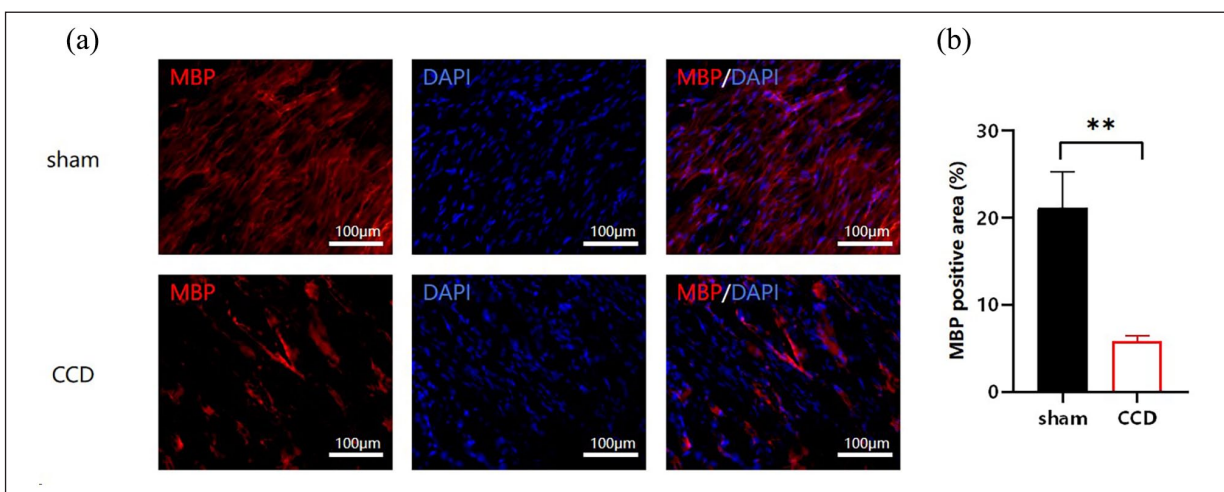


Figure 5. MBP expression in DRG was significantly reduced after the establishment of CCD model: (a) A representative micrograph of MBP immunofluorescence in sham and CCD group and (b) Quantification of MBP positive areas in sham and CCD group. MBP: Myelin basic protein (red); DAPI: nuclear staining (blue); Scale bar = 100 μm; Unpaired *T* test. ** $P < .01$.

on neuropathic pain induced by the CCD model. To our knowledge, this is the first animal study to show that DRG PRF relieves neuropathic pain even though the DRG suffering from persistent chronic compression, and it seems that PRF can repair the ultrastructural damage of chronically compressed DRGs.

Hu et al. were the first to establish the CCD model in which L-shaped stainless steel-rods were inserted into the L5 intervertebral foramen, producing steady compression against the DRG.³⁰ Song et al. improved the model by compressing two DRGs (L4 and L5) instead of one, and the purpose of compressing two DRGs was to increase the number of compressed neurons innervating the plantar surface of the hind paw.¹⁶ Similarly to their results, the rats in our CCD group showed mechanical allodynia and heat hyperalgesia (Figure 2b and d). In addition, we found that the CCD model had cold allodynia assessed by the acetone

evaporation test lasting for 4 weeks (Figure 2c), while their results showed that the foot ipsilateral to the chronic compression elicited a reflex withdrawal to a cotton wisp within 2 weeks. Song XJ et al. observed the signs of spontaneous pain in the CCD model, such as licking of the hind paw on the surgical side, which was accompanied by gentle biting or pulling on the nails with the mouth. We found similar behavior in our CCD group during the experiment (Figure 2a). Our histopathological analysis revealed that chronic DRG compression triggered significant demyelination pathology, characterized by both structural myelin sheath disintegration and molecular-level downregulation of myelin basic protein (MBP) expression - a key marker of myelin structure (Figures 3–5). Hu et al. also demonstrated that the CCD model produced behavioral and electrophysiological changes closely related to low-back pain and radicular pain.³⁰ Therefore, this model may pathophysiologically

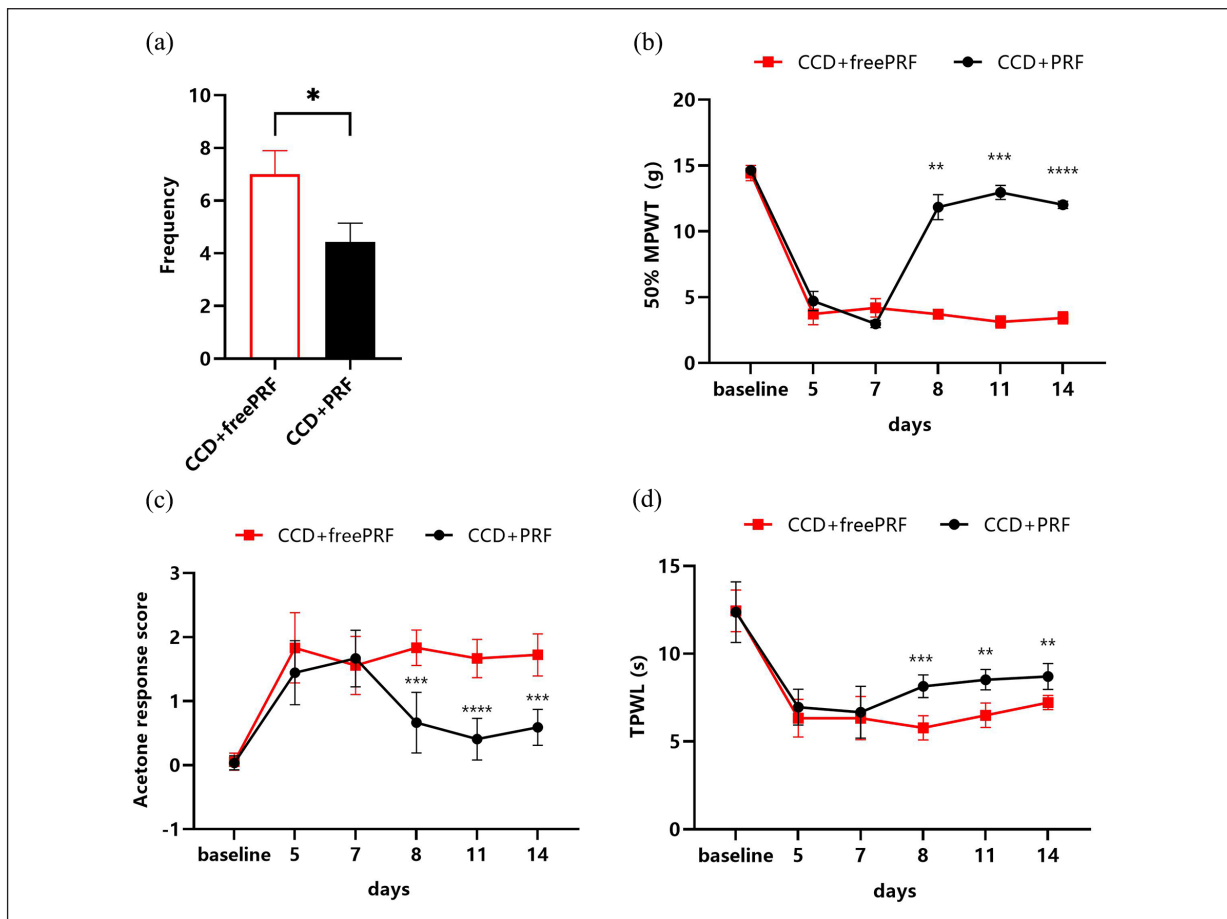


Figure 6. DRG PRF relieves neuropathic pain in CCD rats: (a) PRF alleviates spontaneous pain in CCD rats. $P < .05$; $N = 7/7$; unpaired t -test, (b) Mechanical allodynia relief after PRF treatment. $F(5, 60) = 14.41$; $P < .0001$; $N = 7/7$; Two-way ANOVA with repeated measures and Bonferroni's post-test, (c) Decreased acetone response scores after PRF treatment. $F(5, 60) = 16.27$; $P < .0001$; $N = 7/7$; Two-way ANOVA with repeated measures and Bonferroni's post-test, (d) The thermal paw withdrawal latency increased after PRF treatment. $F(5, 55) = 34.18$; $P < .0001$; $N = 7/7$; Two-way ANOVA with repeated measures and Bonferroni's post-test. * $p < .05$, ** $p < .01$, *** $p < .001$, **** $p < .0001$, MPWT, mechanical paw withdrawal latency; TPWL, thermal paw withdrawal latency.

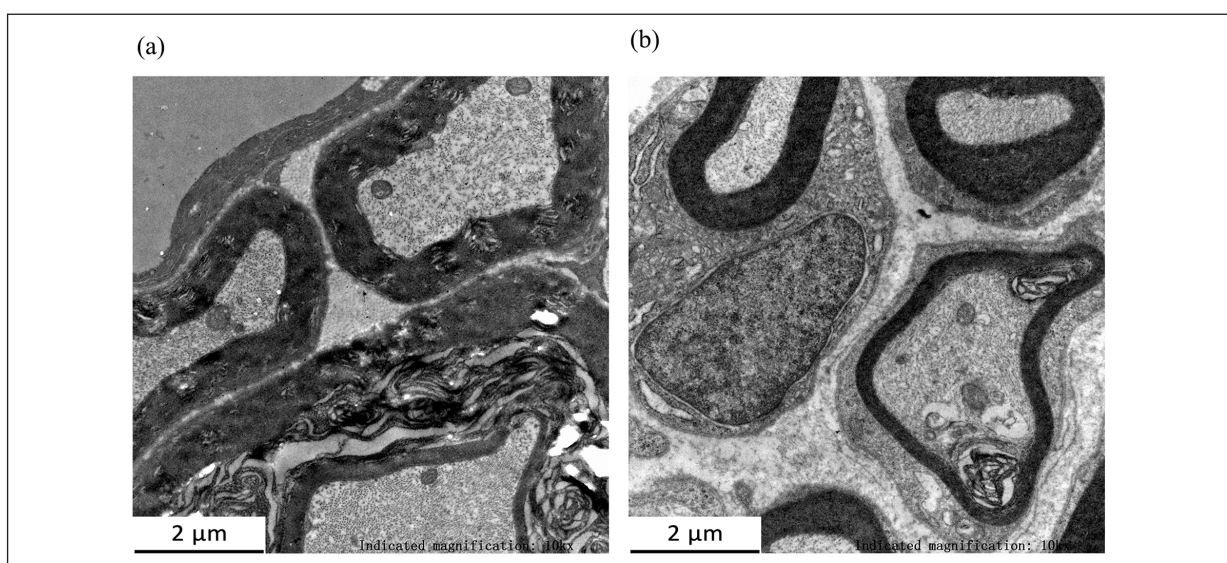


Figure 7. Ultrastructural changes of DRG in CCD+freePRF and CCD+PRF groups: (a) The CCD+freePRF group still had significant myelin damage, such as fracture, stratification, honeycomb and (b) The myelin structure was improved in the CCD+PRF group. Scale bar = 2 μm; magnification *10000.

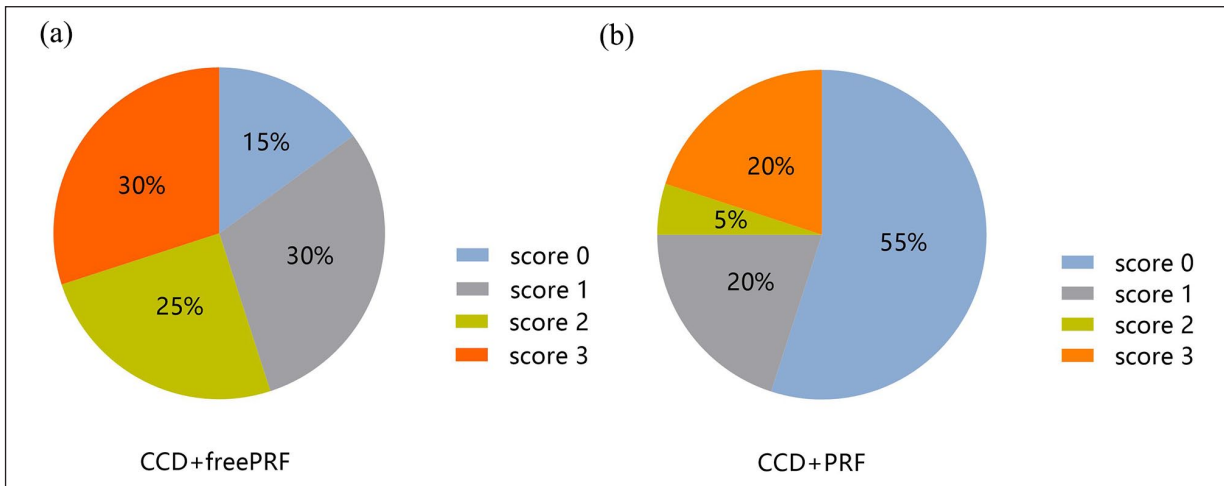


Figure 8. Ultrastructural scores of the CCD+freePRF group (a) and CCD+PRF group (b). $N=20$; $P<.05$. Chi-square.

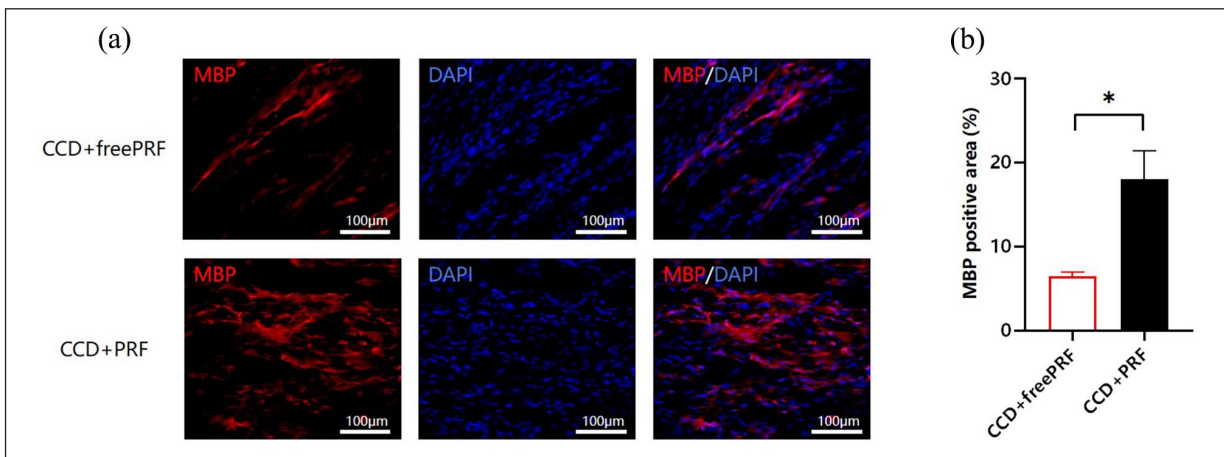


Figure 9. MBP expression increased in DRG after PRF treatment: (a) A representative micrograph of MBP immunofluorescence in CCD+freePRF and CCD+PRF group and (b) Quantification of MBP-positive areas in CCD+freePRF and CCD+PRF group. MBP: Myelin basic protein (red); DAPI: nuclear staining (blue); Scale bar = 100 μm; Unpaired T test. $*P<.05$.

parallel clinical radicular pain syndromes induced by mechanical nerve compression, exemplified by Yang et al.'s characterization of lumbosacral radicular pain secondary to Battered Sensory Nerve Syndrome (BSNS) in patients with foraminal stenosis and post-lumbar instrumented fusion complications.^{9,31}

In clinical practice, many studies confirmed the therapeutic effects of DRG PRF in low-back pain and radicular pain.³²⁻³⁵ Tsou et al. showed that the long-term rate of pain relief in chronic low-back pain with or without lower-limb pain exceeds 50% after applying PRF on the L2 DRG.³⁶ Yang et al. also found that DRG-PRF was effective in relieving lumbosacral radicular pain caused by BSNS.⁹ The previous animal study of PRF on neuropathic pain mainly focused on peripheral nerve injury. Jiang et al. found that the 50% MPWT and TPWL values of the hind paws of CCI rats rose after PRF treatment. However, our research confirms the treatment efficiency of PRF from other insights. Firstly, we provide direct evidence that even under the condition of DRG injury, DRG PRF treatment still had a rapid and satisfying therapeutic effect. Secondly, despite the

DRG suffering consistent compression, the efficiency of one-time DRG PRF lasted for at least 1 week (Figure 6). Thus, it may mean that for DRGs injured by foraminal stenosis or lumbar spine fusion with metal hardware, DRG PRF remains a choice, especially when the compression cannot be solved immediately.

Unlike the classical continuous radiofrequency (CRF) technique, which may cause tissue heating and lead to localized destruction of the neural signaling, pulse radiofrequency can produce analgesic effects under the irreversible tissue destruction threshold.³⁷ A study showed that compared with PRF, CRF induced more fiber destruction, axonal damage and swelling of the mitochondria, meaning that CRF may cause irreversible ultrastructural changes in sciatic nerve fibers.³⁸ However, in our study, we found that PRF can upregulate MBP expression levels, facilitate myelin sheath regeneration and ameliorate the ultrastructural changes in injured ganglia, even under conditions of chronic compression (Figures 7–9). Similar results were found by Li D-Y et al.³⁹ The electron microscope observations revealed that PRF did appear to partially ameliorate

the severe damage induced by CCI. Chen et al. also found that PRF could improve DRG ultrastructure in SNI rats.⁴⁰ A study found that applying PRF to the sciatic nerve not only repaired the myelinated and nonmyelinated nerve fiber structures but could also promote the proliferation of mitochondria.⁴¹ Crucially, mitochondrial dynamics have been implicated as a fundamental determinant of axonal regeneration, given the substantial metabolic demands inherent to neural repair processes.^{42,43} In addition, it has been shown that mitochondrial fission is an acute and adaptive response in injured nerves.⁴⁴ Thus, the efficiency of DRG PRF on unmyelinated C-fibers and nerve fiber mitochondria fission in the CCD model can be explored in the future. Few studies of DRG PRF explore the change in the number of DRG neurons. Shi et al. used stereological methods to find that 54% of DRG neurons were lost in mice after sciatic nerve axotomy, while another study found that the loss of axotomized neurons in rats occurs at a rate of only about 8% per 100 postoperative days.^{45,46} The potential mechanisms of CCD and PRF treatment to the DRG neuron number remain to be studied in the future.

Our research has several limitations that warrant systematic exploration. Firstly, given the well-documented age-dependent decline in remyelination capacity, the exclusion of aged rodent models in the current experimental paradigm necessitates subsequent validation studies to determine whether PRF retains its therapeutic efficacy in senescent microenvironments characterized by compromised myelin repair mechanisms. Secondly, due to the complexity of the mechanisms governing DRG PRF, further research is urgently required to comprehensively investigate its effects on the count and ultrastructural integrity of DRG neurons, as well as other associated cellular components. Finally, addressing the electrophysiological aspects can help understand the role of PRF in repairing DRG ultrastructural damage in the future.

Conclusions

The results of this study revealed that DRG PRF had an analgesic effect on neuropathic pain, even for DRGs suffering persistent compression. The ultrastructural damage of DRGs ameliorated after direct PRF treatment, which may be involved in the mechanism of analgesia.

ORCID iDs

Xuelian Li  <https://orcid.org/0009-0003-4861-5952>

Ying Yang  <https://orcid.org/0009-0002-0097-5505>

Ethical Considerations

The animal study was reviewed and approved by the Laboratory Animal Ethics Committee of Central South University (NO. 2022-0042).

Consent to Participate

Not applicable.

Consent for Publication

Not applicable.

Author Contributions

D.H. and J.M. designed the experiments. X.L. and Y.Y. performed the experiments. J.M. and X.L. analyzed the data. Y.H. wrote the manuscript. All authors have read and agreed to the published version of the manuscript.

Funding

The author(s) disclosed receipt of the following financial support for the research, authorship, and/or publication of this article: This research was funded by the National Natural Science Foundation of China (82271512 to D.H.).

Declaration of conflicting interests

The author(s) declared no potential conflicts of interest with respect to the research, authorship, and/or publication of this article.

Data Availability Statement

The data that support the findings of this study are available from the corresponding author upon reasonable request.

Supplemental material

Supplemental material for this article is available online.

References

- Jensen TS, Baron R, Haanpää M, et al. A new definition of neuropathic pain. *Pain*. 2011;152(10):2204-2205. doi:10.1016/j.pain.2011.06.017
- Moisset X. Neuropathic pain: evidence based recommendations. *Presse Med*. 2024;53(2):104232. doi:10.1016/j.lpm.2024.104232
- Van Boxem K, Huntoon M, Van Zundert J, Patijn J, van Kleef M, Joosten EA. Pulsed radiofrequency: a review of the basic science as applied to the pathophysiology of radicular pain: a call for clinical translation. *Reg Anesth Pain Med*. 2014;39(2):149-159. doi:10.1097/aap.0000000000000063
- Finnerup NB, Kuner R, Jensen TS. Neuropathic pain: from mechanisms to treatment. *Physiol Rev*. 2021;101(1):259-301. doi:10.1152/physrev.00045.2019
- Doth AH, Hansson PT, Jensen MP, Taylor RS. The burden of neuropathic pain: a systematic review and meta-analysis of health utilities. *Pain*. 2010;149(2):338-344. doi:10.1016/j.pain.2010.02.034
- Gilron I, Baron R, Jensen T. Neuropathic pain: principles of diagnosis and treatment. *Mayo Clin Proceed*. 2015;90(4):532-545. doi:10.1016/j.mayocp.2015.01.018
- North RY, Li Y, Ray P, et al. Electrophysiological and transcriptomic correlates of neuropathic pain in human dorsal root ganglion neurons. *Brain J Neurol*. 2019;142(5):1215-1226. doi:10.1093/brain/awz063
- Li X, Zhang H, Zhang X, et al. A central and peripheral dual neuromodulation strategy in pain management of zoster-associated pain. *Sci Reports*. 2024;14(1):24672. doi:10.1038/s41598-024-75890-4
- Yang L, Huang Y, Ma J, et al. Clinical outcome of pulsed-radiofrequency combined with transforaminal epidural steroid

- injection for lumbosacral radicular pain caused by distinct etiology. *Front Neurosci.* 2021;15:683298. doi:10.3389/fnins.2021.683298
10. Chang MC. Efficacy of pulsed radiofrequency stimulation in patients with peripheral neuropathic pain: a narrative review. *Pain Phys.* 2018;21(3):E225-E234.
 11. Jorge DMF, Huber SC, Rodrigues BL, et al. The mechanism of action between pulsed radiofrequency and orthobiologics: is there a synergistic effect? *Int J Mol Sci.* 2022;23(19):1726. doi:10.3390/ijms231911726
 12. Huang RY, Liao CC, Tsai SY, et al. Rapid and delayed effects of pulsed radiofrequency on neuropathic pain: electrophysiological, molecular, and behavioral evidence supporting long-term depression. *Pain Phys.* 2017;20(2):E269-E283.
 13. Schianchi PM, Sluijter ME, Balogh SE. The treatment of joint pain with intra-articular pulsed radiofrequency. *Anesthesiol Pain Med.* 2013;3(2):250-255. doi:10.5812/aapm.10259
 14. Mercadal B, Vicente R, Ivorra A. Pulsed radiofrequency for chronic pain: in vitro evidence of an electroporation mediated calcium uptake. *Bioelectrochemistry.* 2020;136:107624. doi:10.1016/j.bioelechem.2020.107624
 15. Rui M, Han Z, Xu L, Yao M. Effect of CT-guided repeated pulsed radiofrequency on controlling acute/subacute zoster-associated pain: a retrospective cohort study. *Pain tTherapy.* 2024;13(1):99-112. doi:10.1007/s40122-023-00567-1
 16. Liem L, van Dongen E, Huygen FJ, Staats P, Kramer J. The dorsal root ganglion as a therapeutic target for chronic pain. *Reg Anesth Pain Med.* 2016;41(4):511-519. doi:10.1097/aap.0000000000000408
 17. Jiang R, Li P, Yao YX, et al. Pulsed radiofrequency to the dorsal root ganglion or the sciatic nerve reduces neuropathic pain behavior, decreases peripheral pro-inflammatory cytokines and spinal β -catenin in chronic constriction injury rats. *Reg Anesth Pain Med.* 2019;4:32. doi:10.1136/rapm-2018-100032
 18. Shi C, Qiu S, Riester SM, et al. Animal models for studying the etiology and treatment of low back pain. *J Ortho Res Pub Orthopaedic Res Soc.* 2018;36(5):1305-1312. doi:10.1002/jor.23741
 19. Fang X, Xu X, Lin X, Liu R. Downregulated spinal IRF8 and BDNF in NAC are involved in neuropathic pain-induced depression relief via pulsed radiofrequency on dorsal root ganglion in rat SNI model. *Brain Res Bull.* 2019;146:192-200. doi:10.1016/j.brainresbull.2019.01.008
 20. Song XJ, Hu SJ, Greenquist KW, Zhang JM, LaMotte RH. Mechanical and thermal hyperalgesia and ectopic neuronal discharge after chronic compression of dorsal root ganglia. *J Neurophysiol.* Dec 1999;82(6):3347-3358. doi:10.1152/jn.1999.82.6.3347
 21. Kupers RC, Nuytten D, De Castro-Costa M, Gybels JM. A time course analysis of the changes in spontaneous and evoked behaviour in a rat model of neuropathic pain. *Pain.* 1992;50(1):101-111. doi:10.1016/0304-3959(92)90117-t
 22. Dixon WJ. Efficient analysis of experimental observations. *Ann Rev Pharmacol Toxicol.* 1980;20:441-462. doi:10.1146/annurev.pa.20.040180.002301
 23. Chaplan SR, Bach FW, Pogrel JW, Chung JM, Yaksh TL. Quantitative assessment of tactile allodynia in the rat paw. *J Neurosci Methods.* 1994;53(1):55-63. doi:10.1016/0165-0270(94)90144-9
 24. Silva-Cardoso GK, Lazarini-Lopes W, Hallak JE, et al. Cannabidiol effectively reverses mechanical and thermal allodynia, hyperalgesia, and anxious behaviors in a neuropathic pain model: Possible role of CB1 and TRPV1 receptors. *Neuropharmacology.* 2021;197:108712. doi:10.1016/j.neuropharm.2021.108712
 25. Yoon C, Wook YY, Sik NH, Ho KS, Mo CJ. Behavioral signs of ongoing pain and cold allodynia in a rat model of neuropathic pain. *Pain.* 1994;59(3):369-376. doi:10.1016/0304-3959(94)90023-x
 26. Deuis JR, Dvorakova LS, Vetter I. Methods used to evaluate pain behaviors in rodents. *Front Mol Neurosci.* 2017;10:284. doi:10.3389/fnmol.2017.00284
 27. Kaptanoglu E, Palaoglu S, Surucu HS, Hayran M, Beskonakli E. Ultrastructural scoring of graded acute spinal cord injury in the rat. *J Neurosurg.* 2002;97(1 Suppl):49-56. doi:10.3171/spi.2002.97.1.0049
 28. Lin ML, Lin WT, Huang RY, et al. Pulsed radiofrequency inhibited activation of spinal mitogen-activated protein kinases and ameliorated early neuropathic pain in rats. *Eur J Pain.* 2014;18(5):659-670. doi:10.1002/j.1532-2149.2013.00419.x
 29. Perret DM, Kim DS, Li KW, et al. Application of pulsed radiofrequency currents to rat dorsal root ganglia modulates nerve injury-induced tactile allodynia. *Anesth Analg.* 2011;113(3):610-616. doi:10.1213/ANE.0b013e31821e974f
 30. Hu SJ, Xing JL. An experimental model for chronic compression of dorsal root ganglion produced by intervertebral foramen stenosis in the rat. *Pain.* 1998;77(1):15-23. doi:10.1016/s0304-3959(98)00067-0
 31. Gu X, Yang L, Wang S, et al. A rat model of radicular pain induced by chronic compression of lumbar dorsal root ganglion with SURGIFLO. *Anesthesiology.* 2008;108(1):113-121. doi:10.1097/01.anes.0000296073.16972.13
 32. Park S, Park JH, Jang JN, et al. Pulsed radiofrequency of lumbar dorsal root ganglion for lumbar radicular pain: a systematic review and meta-analysis. *Pain Pract J World Instit Pain.* 2024;24(5):772-785. doi:10.1111/papr.13351
 33. Kim CS, Kim Y, Kim DH, Kwon HJ, Shin JW, Choi SS. Effects of pulsed radiofrequency duration in patients with chronic lumbosacral radicular pain: a randomized double-blind study. *Neuromodulation.* 2024;4:6. doi:10.1016/j.neurom.2024.03.006
 34. Mehta V, Snidvongs S, Ghai B, Langford R, Wodehouse T. Characterization of peripheral and central sensitization after dorsal root ganglion intervention in patients with unilateral lumbosacral radicular pain: a prospective pilot study. *Br J Anaesth.* 2017;118(6):924-931. doi:10.1093/bja/aex089
 35. Napoli A, Alfieri G, Scipione R, Andrani F, Leonardi A, Catalano C. Pulsed radiofrequency for low-back pain and sciatica. *Expert Rev Med Dev.* 2020;17(2):83-86. doi:10.1080/17434440.2020.1719828
 36. Tsou HK, Chao SC, Wang CJ, et al. Percutaneous pulsed radiofrequency applied to the L-2 dorsal root ganglion for treatment of chronic low-back pain: 3-year experience. *J Neurosurg Spine.* 2010;12(2):190-6. doi:10.3171/2009.9.Spine08946
 37. Erdine S, Bilir A, Cosman ER, Cosman ER Jr. Ultrastructural changes in axons following exposure to pulsed radiofrequency fields. *Pain Pract J World Institute Pain.* 2009;9(6):407-417. doi:10.1111/j.1533-2500.2009.00317.x
 38. Choi S, Choi HJ, Cheong Y, Chung SH, Park HK, Lim YJ. Inflammatory responses and morphological changes of radiofrequency-induced rat sciatic nerve fibres. *European journal of pain.* 2014;18(2):192-203. doi:10.1002/j.1532-2149.2013.00391.x

39. Li DY, Meng L, Ji N, Luo F. Effect of pulsed radiofrequency on rat sciatic nerve chronic constriction injury: a preliminary study. *Chin Med J*. 2015;128(4):540-544. doi:10.4103/0366-6999.151113
40. Chen R, Xu X, Yu Y, Chen Y, Lin C, Liu R. High-voltage pulsed radiofrequency improves ultrastructure of DRG and enhances spinal microglial autophagy to ameliorate neuropathic pain induced by SNI. *Scientific reports*. 2024;14(1):4497. doi:10.1038/s41598-024-55095-5
41. Dai Z, Xu X, Chen Y, Lin C, Lin F, Liu R. Effects of high-voltage pulsed radiofrequency on the ultrastructure and Nav1.7 level of the dorsal root ganglion in rats with spared nerve injury. *Neuromodulation*. 2022;25(7):980-988. doi:10.1111/ner.13527
42. Han Q, Xie Y, Ordaz JD, et al. Restoring cellular energetics promotes axonal regeneration and functional recovery after spinal cord injury. *Cell metabolism*. 2020;31(3):623-641. doi:10.1016/j.cmet.2020.02.002
43. McElroy T, Zeidan RS, Rathor L, Han SM, Xiao R. The role of mitochondria in the recovery of neurons after injury. *Neural regeneration research*. 2023;18(2):317-318. doi:10.4103/1673-5374.343907
44. Kiryu-Seo S, Tamada H, Kato Y, et al. Mitochondrial fission is an acute and adaptive response in injured motor neurons. *Scientific reports*. 2016;6:28331. doi:10.1038/srep28331
45. Devor M, Govrin-Lippmann R, Frank I, Raber P. Proliferation of primary sensory neurons in adult rat dorsal root ganglion and the kinetics of retrograde cell loss after sciatic nerve section. *Somatosensory research*. 1985;3(2):139-167. doi:10.3109/07367228509144581
46. Shi TJ, Tandrup T, Bergman E, Xu ZQ, Ulfhake B, Hökfelt T. Effect of peripheral nerve injury on dorsal root ganglion neurons in the C57 BL/6J mouse: marked changes both in cell numbers and neuropeptide expression. *Neuroscience*. 2001;105(1):249-263. doi:10.1016/s0306-4522(01)00148-8